The Journal of Phytopharmacology 2024; 13(5):352-358
Online at: www.phytopharmajournal.com

Research Article

ISSN 2320-480X
JPHYTO 2024; 13(5): 352-358
September- October
Received: 08-08-2024
Accepted: 17-10-2024

doi: 10.31254/phyto.2024.13502

Shivani Chauhan
Department of Biotechnology, COH & F, Neri, Dr YS Parmar University of Horticulture and Forestry, Hamirpur, Himachal Pradesh, India

Himani Sharma
Department of Biotechnology, COH & F, Neri, Dr YS Parmar University of Horticulture and Forestry, Hamirpur, Himachal Pradesh, India

Kiran Thakur
Department of Biotechnology, COH & F, Neri, Dr YS Parmar University of Horticulture and Forestry, Hamirpur, Himachal Pradesh, India

Arti Ghabru
Department of Biotechnology, COH & F, Neri, Dr YS Parmar University of Horticulture and Forestry, Hamirpur, Himachal Pradesh, India

Disha Thakur
Department of Fruit Science, KVK Seobagh Dr YS Parmar University of Horticulture and Forestry, Hamirpur, Himachal Pradesh, India

Abhishek Thakur
Department of Biotechnology, COH & F, Neri, Dr YS Parmar University of Horticulture and Forestry, Hamirpur, Himachal Pradesh, India

Poonam
School of Bioengineering and Food Technology, Shoolini University, Solan Himachal Pradesh, India

Correspondence:
Dr. Himani Sharma
Department of Biotechnology, COH & F, Neri, Dr YS Parmar University of Horticulture and Forestry, Hamirpur, Himachal Pradesh, India
Email: sharmahimani8@gmail.com

Mitigating brilliant green dye phytotoxicity through bioiron nanoparticles: Enhancing plant safety and defense

Shivani Chauhan, Himani Sharma, Kiran Thakur, Arti Ghabru, Disha Thakur, Abhishek Thakur, Poonam

ABSTRACT

Nanoparticles due to non-toxicity, bioavailability and efficiency are popular in agriculture. Iron being one of most important micronutrients is essential for growth of plants and their development. In the present study bio prospecting of iron rich sites was carried for quantitative assessment of bioiron nanoparticles synthesizing activity and molecular characterization. The iron nanoparticle synthesized by *Bacillus cereus* strain MJS3.0 were analysed by UV-visible spectroscopy, FTIR, XRD, SEM and DLS techniques. Phytotoxicity studies of one of the most potent textile dye Brilliant green was studied by biosynthesized iron nanoparticles under in vitro and *in vivo* conditions as decolourization does not mean detoxification. Thus, twelve agriculturally important plant species were assessed in relative *in vitro* sensitivity experiments and 100% seed germination along with highest plumule and radical development was observed with iron nanoparticles treated 20 ppm brilliant green dye within 2 weeks of time. In vivo experiments conducted in triplicates determined 100% seed germination and increased shoot and root length, respectively. Thus, iron nanoparticles being environment friendly and cost effective not only leads to protection of human health and maintenance of ecological balance but also remediates contaminants from soil at faster rate and thus lead to plant protection.

Keywords: Iron nanoparticles, Bioprospecting, Brilliant green, Phytotoxicity, *Bacillus cereus*, Plant protection.

INTRODUCTION

Exploring natural resources and the environment for different macromolecules, small compounds, biochemical information and genetic information that may one day be converted into economically useful products for bioremediation, agriculture and nanobiotechnology is known as bioprospecting [1]. Due to its diverse paramagnetism, endurance and antibacterial capabilities, iron nanoparticles are widely employed nowadays [2]. These nanoparticles are easily formed and have a high success rate when produced using microorganisms like bacteria, yeast, fungus, algae, etc. Additionally, bioiron nanoparticles are produced in an environmentally sustainable manner without the use of harmful, costlier poisonous substances. Because iron nanoparticles interact with plants and the environment and accumulate in plant biomass, their usage in agriculture is dependent on their toxicity and overdose rate [3]. When present in the root surface, these iron nanoparticles alter the chemistry of the root, which in turn affects how nutrients are taken up by the plant roots [4]. Furthermore, in hypothetical studies, the pathways through which nanoparticles and their solute are absorbed are hydrophilic compounds, which are absorbed by the aqueous pores of the cuticle, stomata and lipophilic compounds by cuticular diffusion. After dissolving or moving through the cuticle, iron nanoparticles with larger surface areas quickly bind wax lipids and cuticular wax leads to trapping and diffusion of particles in leaf tissues [5]. Large agglomerates are said to have been retained on the surface wax, whereas smaller particles may have been absorbed into the leaf [6].

Wax inducer1 (WIN1), an ethylene response factor type transcription factor, can also trigger wax accumulation at the molecular level by controlling the expression of metabolic pathway genes in plants that over express it [7]. New leaves also turn chlorotic in iron-deficient plants and immature lateral roots exhibit stress response mechanisms such as sub-apical swelling, increased Fe (III) reduction capacity and medium acidity. When a plant lacks iron, its reductive mechanism is triggered, the FRO_2 gene codes for a ferric chelate reductase. As a result, plants benefit from the foliar application of iron nanoparticles in the form of $Fe2O_3$ and Fe^{3+}, which stimulates plant growth and development. It's been reported in several studies that root applied iron oxide nanoparticles (γ-Fe_2O_3) have positive effects on plant growth. [8] reported effectiveness of iron nanoparticles on germination rate, germination percent of seeds, and seedlings development of *Arachis hypogaea*. [9] reported that carbon coated iron nanoparticles were capable of penetrating pumpkin (*Cucurbita pepo* L.) leaves and migrating to other plant tissues. Iron nanoparticles showed a significant effect on seedling development and shoot growth.

Biologically synthesized iron nanoparticles enhanced root elongation of *Lactuca sativa* seedlings by 12-26%, indicating that iron nanoparticles could be used as iron fertilizer at low application rates (5-20 ppm)[10].

As compared to plants grown from control seeds and biomass enhancement of *Spinacia oleracea*, the use of iron nanoparticles resulted in improved leaf shape, greater biomass, bigger leaf numbers and chemical characteristics (higher concentration of calcium, zinc, and manganese in the leaves). In seeds treated with iron nanoparticles, there is an accelerated breakdown of stored starch, leading to noticeably greater growth [11]. According to [12], iron oxide nanoparticles (Fe_2O_3) increased the root length, plant height, biomass, and chlorophyll levels of *Arachis hypogaea* plants, suggesting that they might be used in place of conventional iron fertilizers when growing *Arachis hypogaea* plants.

In order to conduct bioprospecting of iron nanoparticle synthesizing activities and assess the phytotoxicity of brilliant green for plant protection, the research was designed with the aforementioned factors in mind.

MATERIALS AND METHODS

Isolation of Iron Nanoparticle-Producing Bacteria

In a survey, bacteria that synthesize iron nanoparticles were isolated from several sites in the Himachal Pradesh districts of Mandi and Kangra. Four locations in all, Sangalwara and Jhungi in the Mandi district and Bir and Kothi Kodh in the Kangra district, were chosen. (Table 1) displays the locations of these sites together with their altitudes (m).

Table 1: Geographical location of selected sites

S. No.	District	Site	Site Code	Sample codes	Altitude (m)
1	Kangra	Bir	KB	KBS1	32°03':76'47
				KBS2	
				KBW1	
				KBW2	
				KBP1	
				KBP2	
2	Kangra	Kothi Kodh	KK	KKS1	35º05':76'52'
				KKS2	
				KKW1	
				KKW2	
				KKP1	
				KKP2	
3	Mandi	Sangalwaro	MS	MSS1	31º30':77'13'
				MSS2	
				MSW1	
				MSW2	
				MSP1	
				MSP2	
4	Mandi	Jhungi	MJ	MJS1	31º25':77'06'
				MJS2	
				MJW1	
				MJW2	
				MJP1	
				MJP2	

Synthesis of Bioiron Nanoparticles

112 bacterial strains from a previous study were evaluated individually for their ability to synthesise iron nanoparticles. A one percent concentration of inoculum (overnight culture) was added to nutrient broth and the combination was then incubated at 30°C for 24 hours at 150 rpm to produce iron nanoparticles. To study the formation of iron nanoparticles, the supernatant was collected by centrifugation at 10,000 rpm, 4°C for 15 minutes. Ten ml of each collected supernatant were combined with ten ml of a 2.0 mM Ferrous sulphate ($FeSO_4$) solution and incubated at 36°C for up to 90 hours. The test tube's colour changed from pale yellow to orange indicating, formation of iron nanoparticles. This colour change was later confirmed by measuring the solution's O.D. value at a wavelength of 350 nm. An empirical observation was also made by aligning the bacteria that produce iron nanoparticles in the media towards an external magnetic field by placing a magnet close to the test tube. Based on the results of this experiment, bacterial isolates with the highest extracellular iron nanoparticle synthesis activity were chosen for additional testing.

Molecular Analysis

Using 16S rRNA gene technology, further molecular analysis of bacterial isolates with the highest extracellular iron nanoparticle synthesis activity was done. The PCR amplification was performed in 0.2 ml PCR tubes with a reaction volume of 20µl with the following ingredients: Taq DNA polymerase (5U/l), Primer F (10nM), Primer R (10nM), template DNA, PCR buffer (10x), $MgCl_2$ (1.5 mM) and a combination of dNTPs (0.5 mM each). The conventional temperature profile included 35 cycles of denaturation at 95ºC for 90 seconds, annealing at 50ºC for 60 seconds, extension at 72 ºC for 90 minutes and final extension at 72ºC for 10 minutes. Universal primers used were:

B27F 5`-AGAGTTTGATCCTGGCTCAG-3'
U1492R 5`-GGTTACCTTGTTACGACTT-3'

The test isolates amplified PCR products were resolved by electrophoresis using a 1.2% agarose gel in a 1X Tris-acetate EDTA buffer (ethidium bromide (0.5 g/ml) and 2M Tris base, 57.10 ml acetic acid and 0.5 M EDTA (pH 8.0, 50X)). A 1 kb DNA ladder was utilized as a marker. The gel was operated on the Bangalore Genei power system at 80 V for a couple of hours. With the help of the gel documentation system, the gel was inspected and a photograph was taken (AlphaImager 2200, Alpha Infotech Corporation, USA). The PCR products produced by amplification using universal primers directed at the 16S rRNA gene were submitted to Merck lab in India for sequencing using the identical upstream and downstream primers. For identification purpose, further *insilico* techniques such as BLASTn, MSA and phylogenetic tree analysis were used.

Characterization of Bioiron Nanoparticles

The procedure of lyophilization was used to prepare bioiron nanoparticles in powdered form. One hundred ml suspension of bioiron nanoparticles were transferred to two petriplates, which were then placed in the lyophilizer chamber (BIOGENTEK (I) Pvt Ltd) for lyophilization, which involves freezing the bioiron nanoparticle solution at30 °C for 48 hours and then lowering the pressure to allow the frozen water to sublime directly from the liquid phase to the gas phase. Several methods, including UV-visible spectroscopy, Fourier Transform Infrared Spectroscopy (FTIR), X-ray diffractions (XRD), field emission scanning electron microscopy (FESEM) and dynamic light scattering, were used to analyse iron nanoparticles produced by bacterial growth. (DLS).

Phytotoxicity studies

In order to assess the toxicity of a particular dye based on its highest percent decolourization value, a phytotoxicity experiment was conducted. Bioiron nanoparticle preparation was applied to the

selected dye in three replications. For this experiment, a standardized concentration of selected dye was dissolved in sterilized distilled water, to investigate its phytotoxicity effects on twelve plant species viz., *Cicer arietinum*, *Cicer kabulianum*, *Spinacia oleracea*, *Cosmos bipinnatus*, *Solanum lycopersicum*, *Viola tricolor*, *Vigna radiata*, *Zinnia elegans*, *Calendula officinalis*, *Brassica juncea*, *Phaseolus vulgaris* and *Raphanus sativus* important in Indian agriculture. The impact of a particular dye and its degradative metabolites on the germination and seedling development of the associated plant species was assessed *in vitro* and *in vivo*. For investigations on phytotoxicity, the original dye solution and the dye solution that had been altered by the addition of bioiron nanoparticles were compared. For *in vitro* studies, seeds were surface sterilized using 0.1% tween20 for 2 minutes, thoroughly rinsed three to four times with sterilized distilled water to remove any remaining 0.1% tween20, then dipped in distilled water, the original dye solution and dye treated with bioiron nanoparticles preparation for 4 hours. Separate seeds were grown in sterile petri plates with sterile filter paper on top. The phytotoxicity investigation was conducted at room temperature by routinely watering the seeds with the appropriate solutions individually and seeds that germinated in petridish treated with water were utilized as a control. For time period, all of the treatments percentages of germination, lengths of plumules (shoots) and radicles (roots) in centimeters, and for *in vivo* studies, five seeds were sown per pot at equidistance and at uniform depth in the soil. To evaluate the phytotoxic effect of selected dye on germination and growth, seeds of each plant species (five seeds per pot) were treated with respective solutions separately *viz*., distilled water, original dye solution and dye treated with iron nanoparticles preparation. Germination of seedlings in pots irrigated with water was taken as control. Length of shoot (cm) and root (cm) of all the treatments were recorded for period of two weeks [6] and percent germination was calculated using following formula:

$$\text{Percent Seed germination} = \frac{\text{Number of seeds germinated}}{\text{Total number of seeds}} \times 100$$

RESULTS AND DISCUSSION

Using nutrient agar (pH 7.0) at an incubation temperature of 30°C for 24 hours, a total of 112 putative iron nanoparticles synthesizing bacterial isolates were isolated from various chosen sites around Himachal Pradesh. Some Thermo anaerobacter species TOR-39 strains have been isolated from sediments and water collected from a range of habitats, such as deep subterranean sediments or hydrothermal vents in the ocean. These strains are capable of synthesizing iron nanoparticles [13]. Additionally, [14] reported the isolation of *Escherichia coli* producing iron nanoparticles from soil samples. According to [15], *Bacillus subtilus* that produces iron nanoparticles was isolated from the soil rhizosphere. *Thiobacillus thioparus* was identified from the soil of several iron ore mining locations in India by [16]. [17] from Aran Bidgol lake seabed soil and Zamankhan river water samples from Isfahan, Iran. Maximum iron nanoparticles with an OD value of 0.98 and a wavelength of 350 nm were created at pH 8.0. Using universal primers, the DNA sample of the bacterial isolate that produces the most iron nanoparticles was selectively amplified using PCR technology. After 35 cycles of PCR amplification, amplicons of the anticipated size, or 1500 bp, were created. Bacillus isolate MJS3.0's 16S rRNA gene sequence analysis revealed 99% identity with the whole 16S ribosomal RNA sequence of *Bacillus cereus* and was therefore identified as the MJS3.0 strain.

Characterization of iron nanoparticles

Several methods were used to characterise these iron nanoparticles, including UV-Vis spectroscopy, which revealed a spectrum of peaks at 350 nm, which is typical of iron nanoparticles. (Figure 1). From the first at a wavelength of 3287.66 cm^{-1} to the eighth at a wavelength of 552.56 cm, the FTIR pattern of the production of iron nanoparticles is shown in (Figure 2). An extracellular production of iron nanoparticles employing *Bacillus cereus* strain MJS3.0 to reduce ferrous sulphate ions was clearly demonstrated by the XRD pattern in Figure 1c. Iron nanoparticle generation was observed by broad peaks at a 2 value of 33°. The Scherer equation was used to determine the crystal size (Figure 3).

$$D = K\lambda/\beta Cos\theta$$

Where λ= wavelength of incident ray (1.5418Å)
K= shape factor (0.9)
θ is the Bragg angle
β = isbroadening line at half the maximum intensity (FWHM), also denoted as 2θ
D = Mean size of the ordered (crystalline) domains

According to the XRD pattern, the average crystal size, Dwas around 1.82376 nm and the average crystal particle size is close to 45.5 nm. According to a dynamic light scattering (DLS) graph, iron nanoparticles had an average diameter of 80 nm and30% intensity (Figure 4). Results from scanning electron microscopy (SEM) showed that iron nanoparticles were mono dispersed and had a triangular shape (Figure 5). In a different study [9], iron nanoparticles were characterized by UV-visible spectroscopy, TEM and SEM. It was discovered that the nanoparticles maximum absorbance was between 250 and 350 nm in UV-Vis spectroscopy, and that TEM and SEM micrographs showed spherical nanoparticles between 60 and 80 nm in size. The characterization of nanoparticles using UV-Vis, X-ray diffraction and SEM was reported by [17]. Maximum absorbance was seen in UV-Vis spectroscopy at wavelengths of 283 nm and 368 nm, the acquired XRD spectrum at 2θ values of 35.6 ° and 45.6 °; and the SEM picture revealed that the biosynthesized iron nanoparticles were 100-200 nm in size. Using UV-scanning spectroscopy and TEM, [18] characterized iron nanoparticles. An absorption peak at 267 nm was identified, and the TEM results showed that the iron nanoparticles were irregular in form and ranged in size from 20 to 25 nm. Iron nanoparticles were characterized by [19] using TEM and UV-visible spectroscopy. The UV-visible spectroscopy revealed the iron nanoparticles to be monodispersed with a size range of 1.4-2.8nm, while TEM micrographs revealed maximum absorbance at 400-464nm. Similar to this, [20] used SEM and UV-visible spectroscopy to characterize iron nanoparticles.

Phytotoxicity assay by bioiron nanoparticles

As decolourization of dyes does not necessarily imply detoxification, it is crucial to assess the phytotoxicity of textile dyes. To do this, toxicity assays using biosynthesized iron nanoparticles was carried out to compare the phytotoxicity of Brilliant Green dye before and after degradation. Twelve agriculturally significant plant species, including *Zinnia elegans*, *Calendula officinalis*, *Brassica juncea*, *Phaseolus vulgaris* and *Raphanus sativus*, have been studied in relation to the application of biosynthesized iron nanoparticles treated brilliant green dye, water (control) and brilliant green dye as such. To evaluate toxicity, criteria such as the plumule length, radicle length, and percent germination have been utilized [21]. The relative susceptibility of these twelve plant species to brilliant green dye and brilliant green dye coated with iron nanoparticles in comparison to water control was studied both *in vitro* and *in vivo*.

Water was used as the reference control because it showed the highest percentage of germination in plant species when *in vitro* conditions were used, whereas brilliant green dye treatment showed seed germination rates of 30, 40, 65, 40, 70, 40, 45, 60, 40, 65, 50 and 60% for all plant species after two weeks. As opposed to previous treatments, bioiron nanoparticles with brilliant green dye caused 100% seed germination for all twelve species of plants, demonstrating enhanced germination rates. Additionally, it was shown that when seeds were treated with Brilliant green dye, the average length of the plumule and radicle of all twelve plant species was significantly shortened. However, brilliant green dye treated with bioiron nanoparticles demonstrated an increase in length (Table 2).

In *in vivo* experiment, it was shown that using water as the reference control resulted in 100% of seeds germinating in each plant species. However, following two weeks of *in vivo* treatment with brilliant green dye, less seed germination was seen. As a result, 75, 85, 60, 85, 75, 90, 65, 70, 40, 60, 50and 39.5% of the seeds were found to be inhibited from germinating, showing that the brilliant green dye is harmful to plants. As opposed to this, higher levels of seed germination were seen for twelve plants treated with iron nanoparticles instead of brilliant green dye, indicating increased germination rates (Table 3).

All twelve plant species average shoot and root lengths revealed a lowered and slowed rate of growth after being watered with Brilliant Green dye. However, Brilliant green dye treated with iron nanoparticles shown enhanced development (Table 3). Since most azo dyes coexist in industrial waste water, are released into the environment through waste water and have an adverse impact on the entire ecosystem, bioiron nanoparticles produced by *Bacillus cereus* strain MJS3.0 have thus emerged as a potential agent for the detoxification of brilliant green dye. Because bioiron nanoparticles are environmentally safe, cost-effective and help remediate pollutants, their use not only protects human health and ecological balance but also helps remove harmful toxins from soil and waste water.

Table 2: Phytotoxicity effect of Brilliant green dye on seed germination and growth of plants under *in vitro* conditions

S. No.	Plant Species	Parameter studied	Treatments *(In vitro)*		
			Water	Dye	Dye + Iron nanoparticles
1.	***Cicer Arietinum***	Germination (%)	100.0	30.0	100.0
		Plumule (cm)	7.0	3.5	6.9
		Radicle(cm)	5.0	1.0	5.0
2.	***Cicer kabulianum***	Germination (%)	100.0	40.0	100.0
		Plumule (cm)	7.5	3.0	7.0
		Radicle(cm)	4.5	1.5	4.0
3.	***Spinacia oleracea***	Germination (%)	100.0	65.0	100.0
		Plumule (cm)	5.0	2.0	5.0
		Radicle(cm)	6.5	2.5	6.0
4.	***Cosmos bipinnatus***	Germination (%)	100.0	40.0	100.0
		Plumule (cm)	5.6	2.1	5.5
		Radicle(cm)	1.5	0.5	1.2
5.	***Solanum lycopersicum***	Germination (%)	100.0	70.0	100.0
		Plumule (cm)	4.0	2.0	4.0
		Radicle (cm)	3.0	1.0	3.0
6.	***Viola Tricolor***	Germination (%)	100.0	40.0	100.0
		Plumule (cm)	1.7	0.5	1.5
		Radicle(cm)	2.7	1.4	2.6
7.	***Vigna Radiata***	Germination (%)	100.0	45.0	100.0
		Plumule (cm)	3.5	0.6	3.2
		Radicle (cm)	1.4	0.3	1.2
8.	***Zinnia Elegans***	Germination (%)	100.0	60.0	100.0
		Plumule (cm)	2.5	0.6	2.3
		Radicle (cm)	4.1	2.0	4.0
9.	***Calendula officinalis***	Germination (%)	100.0	40.0	100.0
		Plumule (cm)	2.5	1.0	2.3
		Radicle (cm)	5.0	2.0	5.0
10.	***Brassica Juncea***	Germination (%)	100.0	65.0	100.0
		Plumule (cm)	3.0	1.0	3.0
		Radicle(cm)	2.5	0.5	2.4
11.	***Phaseolus vulgaris***	Germination (%)	100.0	50.0	100.0
		Plumule (cm)	2.4	1.0	2.3
		Radicle(cm)	1.7	0.4	1.6
12.	***Raphanus Sativus***	Germination (%)	100.0	60.0	100.0
		Plumule (cm)	6.6	3.2	6.5
		Radicle(cm)	7.5	4.3	7.4

Table 3: Phytotoxicity effect of Brilliant green dye on seed germination and growth of plants under *in vivo* conditions after two weeks

S. No.	Plant Species	Parameter studied	Treatments *(In vivo)*		
			Water	Dyes	Dye + Iron nanoparticles
1.	*Cicer arietinum*	Germination (%)	100.0	25.0	100 .0
		Shoot (cm)	13.0	7.1	12.5
		Root (cm)	6.6	1.8	6.5
2.	*Cicer kabulianum*	Germination (%)	100.0	15.0	100.0
		Shoot (cm)	16.0	10.5	15.8
		Root (cm)	5.4	2.1	5.0
3.	*Spinacia oleracea*	Germination (%)	100.0	40.0	100.0
		Shoot (cm)	18.0	8.5	17.0
		Root (cm)	8.0	3.9	7.8
4.	*Cosmos bipinnatu*	Germination (%)	100.0	15.0	97.5
		Shoot (cm)	12.5	7.0	11.5
		Root (cm)	3.5	1.0	3.4
5.	*Solanum lycopersicum*	Germination (%)	100.0	25.0	80.5
		Shoot (cm)	28.5	10.4	28.0
		Root (cm)	2.5	1.7	2.5
6.	*Viola tricolor*	Germination (%)	100.0	10.0	100.0
		Shoot (cm)	17.5	6.5	17.4
		Root (cm)	6.2	1.5	6.0
7.	*Vigna radiata*	Germination (%)	100.0	35.0	100.0
		Shoot (cm)	9.5	3.6	9.0
		Root (cm)	4.0	1.0	3.9
8.	*Zinnia elegans*	Germination (%)	100.0	30.0	97.0
		Shoot (cm)	5.6	1.0	5.4
		Root (cm)	2.0	0.5	1.8
9.	*Calendula officinalis*	Germination (%)	100.0	60.0	100.0
		Shoot (cm)	14.1	7.0	14.0
		Root (cm)	4.0	1.5	4.0
10.	*Brassica juncea*	Germination (%)	100.0	40.0	100.0
		Shoot (cm)	10.9	5.2	10.4
		Root (cm)	5.5	1.5	5.3
11.	*Phaseolus vulgaris*	Germination (%)	100.0	50.0	95.0
		Shoot (cm)	15.2	10.6	14.2
		Root (cm)	4.9	1.6	4.6
12.	*Raphanus sativus*	Germination (%)	100.0	60.5	100.0
		Shoot (cm)	12.5	9.5	12.5
		Root (cm)	6.4	2.5	6.3

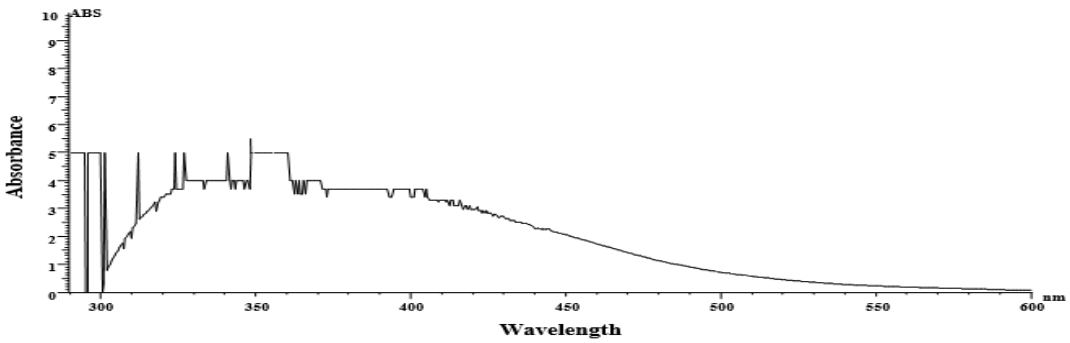

Figure 1: UV-Vis spectra of iron nanoparticles synthesized by *Bacillus cereus* strain MJS 3.0

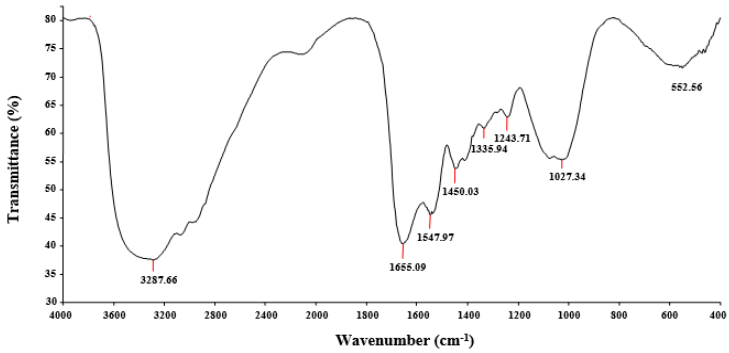

Figure 2: FTIR spectra of iron nanoparticles synthesized by *Bacillus cereus* strain MJS 3.0

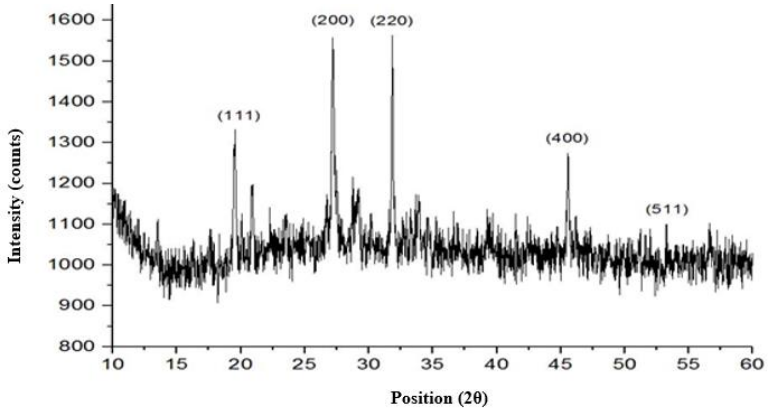

Figure 3: XRD spectra of iron nanoparticles synthesized by *Bacillus cereus* strain MJS 3.0

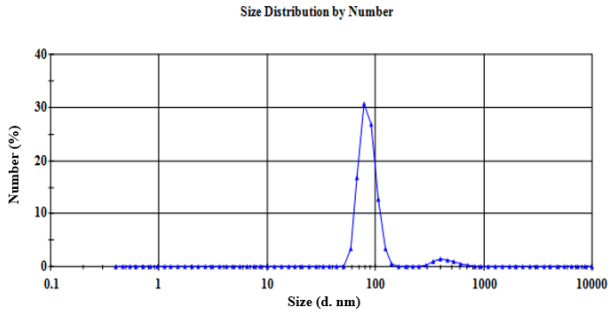

Figure 4: DLS analysis of iron nanoparticles synthesized by Bacillus cereus strain MJS 3.0

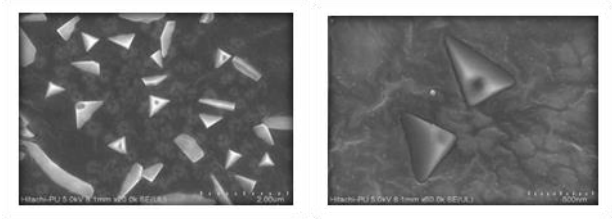

Figure 5: SEM images showing aggregates of iron nanoparticles and their size

CONCLUSION

This research highlights the effectiveness of bioiron nanoparticles in reducing the harmful effects of Brilliant Green dye on plants. By enhancing plant defense mechanisms and improving growth, bioiron nanoparticles offer a promising solution to mitigate dye-induced toxicity. These nanoparticles help boost the activity of antioxidant enzymes, reduce oxidative damage and support nutrient uptake, leading to healthier plant development despite the presence of the dye. Bioiron nanoparticles contribute to maintain a stable internal environment in plants, minimizing the adverse effects of brilliant green on root and shoot growth. This approach presents a sustainable and environmentally friendly method to combat dye pollution while increasing plant resilience. Future research should investigate long-term impacts and the application of this strategy across a variety of plant species to maximize its potential for broader agricultural and environmental applications.

Acknowledgements

Authors are thankful to Panjab University, Chandigarh (India) and Institute of Nano Science and Technology (INST), Mohali (India) for providing laboratory for nanoparticles studies.

Conflict of interest

The authors declared no conflict of interest.

Financial Support

None declared.

ORCID ID

Himani Sharma: https://orcid.org/0000-0003-0256-2114

Kiran Thakur: https://orcid.org/0000-0002-9685-4144

Arti Ghabru: https://orcid.org/0000-0001-9311-1591

Disha Thakur: https://orcid.org/0009-0003-7017-783X

Abhishek Thakur: https://orcid.org/0000-0003-4937-9253

Poonam: https://orcid.org/0000-0001-7546-7834

REFERENCES

1. Beattie AJ, Barthlott W, Elisabetsky E. New products and industries from biodiversity. In: Hassan R, Scholes R, Ash N, editors. Ecosystems and Human Well-Being. Millennium Ecosystem Assessment, Island Press; Washington D.C: 2005; 273–95.
2. Ajinkya N, Yu X, Kaithal P, Luo H, Somani P, Ramakrishna S. Magnetic iron oxide nanoparticle (IONP) synthesis to applications: Present and future. Materials 2020;13:4644.
3. Mohamad Rodzi US, Kiew PL, Lam MK, Tan LS. A feasibility study on the green synthesis of iron oxide nanoparticles using Chlorella vulgaris extract for photocatalytic degradation of crystal violet. IOP Conference Series: Earth and Environmental Science 2023;1144:012004.
4. Wang X, Xie H, Wang P, Yin H. Nanoparticles in Plants: Uptake, Transport and Physiological Activity in Leaf and Root. Materials (Basel) 2023;16(8):3097.
5. Perez-de-Luque A. Interaction of Nanomaterials with Plants: What Do We Need for Real Applications in Agriculture? Frontiers in Environmental Science2017;5:12.
6. Tripathi D K, Shweta, Singh S, Singh S, Pandey R, Singh V P, Sharma N C, Prasad S M, Dubey N K, Chauhan D K. An overview on manufactured nanoparticles in plants: Uptake, translocation, accumulation and phytotoxicity. Plant Physiology and Biochemistry 2017;110:2–12.
7. Broun P. Transcription factors as tools for metabolic engineering in plants. Current Opinion and Plant Biology 2004;7: 202–209.
8. Ding H, Duan LH, Wu HL, Yang RX, Ling HQ Li WX. Regulation of AhFRO1, an Fe (III)-chelate reductase of peanut, during iron deficiency stress and intercropping with maize. Journal of Plant Physiology 2009; 3: 274-283.
9. Corredor E, Testillano PS, Coronado MJ, Gonzalezmelendi P, Fernandezpacheco R, Marquina C. Nanoparticle penetration and transport in living pumpkin plants: in situ subcellular identification. BMC Plant Biology 2009; 9:45-55.
10. Srivastava G, Das CK, Das A, Singh SK, Roy M, Kim H, Sethy N, Kumar A, Sharma SK, Singh, RK, Philip D Das M. Seed treatment with iron pyrite (FeS2) nanoparticles increases the production of spinach. RSC Advances 2014; 102: 58495-58504.
11. Rui MM, Ma CX, Hao Y, Guo J, Rui YK, Tang XL, Zhao Q, Fan X, Zhang ZT, Hou TQ, Zhu, SY. Iron oxide nanoparticles as a potential iron fertilizer for peanut (Arachis hypogaea). Frontiers in Plant Science 2016; 7: 1-10.
12. Parshetti G, Kalme S, Saratale G, Govinndwar S. Biodegradation of malachite green by Kocuria rosea MTCC 1532. Acta Chimica Slovencia 2006; 53:492–498.
13. Moon W, Claudia J, Adam J, Rondinone L, Robert T, Phelps J. Large-scale production of magnetic nanoparticles using bacterial fermentation. Indian Journal of Microbiology Biotechnology 2010; 37: 1023-1031.
14. Chatterjee S, Bandyopadhyay A, Sarkar K. Effect of iron oxide and gold nanoparticles on bacterial growth leading towards biological application. Journal of Nanobiotechnology 2012; 9: 34-41.
15. Sundaram AP, Augustine R, Kannan, M. Extracellular biosynthesis of iron oxide nanoparticles by Bacillus subtilis strains isolated from rhizosphere soil. Biotechnology Bioprocess Enggineering 2012; 17: 835-840.
16. Elcey CD, Kuruvilla AT, Thomas D. Synthesis of magnetite nanoparticles from optimized iron reducing bacteria isolated from iron ore mining sites. International Journal of Current Microbiology and Applied Science 2014; 3(8): 408-417.
17. Gholampoor N, Emtiazi G, Emami, Z. The influence of Microbacterium hominis and Bacillus licheniformis extracellular polymers on Iron and iron oxide nanoparticles production; green biosynthesis and mechanism of bacterial nano production. Journal of Nanomaterial Molecule and Nanotechnology 2015;4: 215-220.
18. Eltarahony M, Zaki S, Kheiralla Z, Haleem D. Biogenic synthesis of iron oxide nanoparticles via optimization of nitrate reductase enzyme using statistical experimental design. Journal of Advanced Biotechnology 2016; 5: 2348-6201.
19. Nath D, Kumar A, Gupta K, Mandal M. Phytosynthesized iron nanoparticles: effects on fermentative hydrogen production by Enterobacter cloacae DH-89. Bulletein Material Science 2016; 38(6): 1533-1538.
20. Vignesh V, Sathiyanarayanan G, Sathishkumar G, Parthiban K, Kumard S, Ramasamy. Formulation of iron oxide nanoparticles using exopolysaccharide: evaluation of their antibacterial and anticancer activities. RSC Advances 2015; 5: 27794-27804.
21. Islam MM, Habib ASM, Parvin F, Rahman MF, Saadat AHM Khan MA. Removal of Industrial dye effluent (Drimarene Yellow) by renewable natural resources. American Acadamy Scholor Research Journal 2013; 5(2): 144-150.

HOW TO CITE THIS ARTICLE

Sharma H, Chauhan S, Thakur K, Ghabru A, Thakur D, Thakur A, Poonam. Mitigating brilliant green dye phytotoxicity through bioiron nanoparticles: Enhancing plant safety and defense. J Phytopharmacol 2024; 13(5):352-358. doi: 10.31254/phyto.2024.13502